Mem. S.A.It. Vol. 81, 625
© SAIt 2010
Memorie della

On the 3D structure of the magnetic field in regions of emerging flux

A. Asensio Ramos[1,2] and J. Trujillo Bueno[1,2,3]

[1] Instituto de Astrofísica de Canarias, 38205, La Laguna, Tenerife, Spain
e-mail: [aasensio;jtb]@iac.es
[2] Departamento de Astrofísica, Universidad de La Laguna, 38205, Tenerife, Spain
[3] Consejo Superior de Investigaciones Científicas, Spain

Abstract. We explore the photospheric and chromospheric magnetic field in an emerging flux region. An image of the equivalent width of the He I 10830 Å red blended component shows the presence of filamentary structures that might be interpreted as magnetic loops. We point out that the magnetic field strength in the chromosphere resembles a smoothed version of that found in the photosphere and that it is not correlated at all with the above-mentioned equivalent width map. Lacking other diagnostics, this suggests that one cannot discard the possibility that the chromospheric field we infer from the observations is tracing the lower chromosphere of the active region instead of tracing the magnetic field along loops. If the He I line is formed within magnetic loops, we point out a potential problem that appears when interpreting observations using only one component along the line-of-sight.

Key words. Sun: activity – Sun: chromosphere — Sun: magnetic fields

1. Introduction

Measuring magnetic fields at chromospheric and coronal heights is notoriously difficult (e.g., the reviews by Harvey 2006; Casini & Landi Degl'Innocenti 2007; Lagg 2007; Trujillo Bueno 2009). There are two fundamental reasons for this. First, the number of lines with diagnostic potential is very scarce. Second, obtaining physical information from the observed spectral line polarization is complex, because chromospheric lines are often dominated by scattering and they are sensitive to magnetic fields not only through the Zeeman effect but also through the modification of the atomic level polarization by the Hanle effect.

In particular, the lines of neutral helium at 10830 Å and 5876 Å (D_3 multiplet) are of great interest for empirical investigations of the dynamic and magnetic properties of plasma structures in the solar chromosphere and corona, such as active regions (e.g., Harvey & Hall 1971; Rüedi et al. 1996; Lagg et al. 2004; Centeno et al. 2006), filaments (e.g., Lin et al. 1998; Trujillo Bueno et al. 2002), prominences (e.g., Landi Degl'Innocenti 1982; Querfeld et al. 1985; Bommier et al. 1994; Casini et al. 2003; Merenda et al. 2006) and spicules (e.g., Trujillo Bueno et al. 2005; Socas-Navarro & Elmore 2005; López Ariste & Casini 2005; Ramelli et al.

Send offprint requests to: A. Asensio Ramos

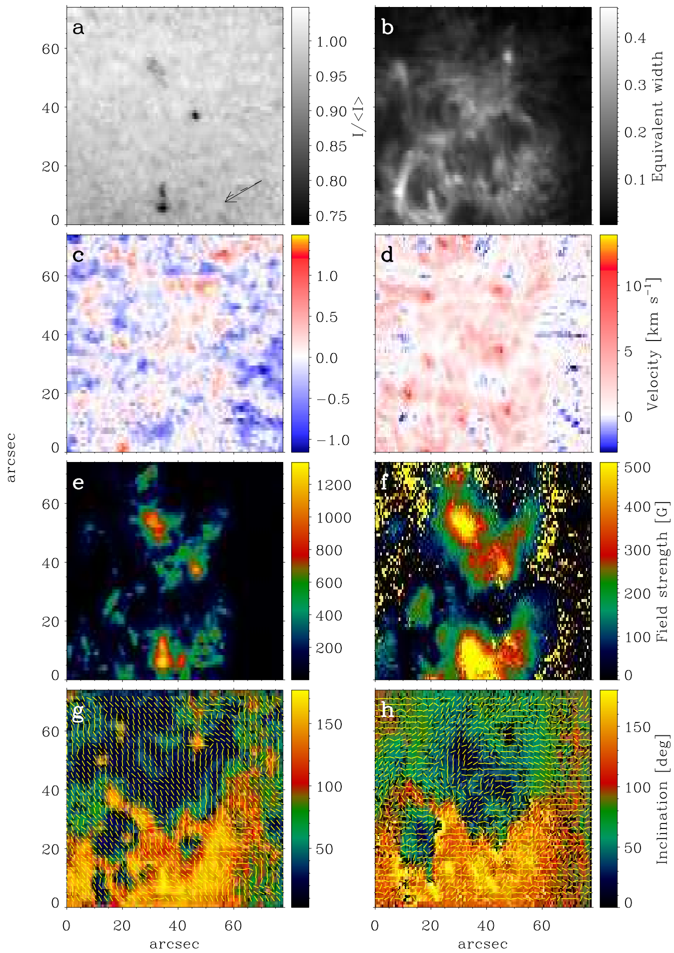

Fig. 1. Photospheric and chromospheric atmospheric parameters: (a) continuum image, (b) image of the equivalent width of the He I red component, showing loop-like filamentary structures, (c) photospheric velocity field, (d) chromospheric velocity field, showing strong downflows close to the footpoints of the loop-like structures seen in the equivalent width image, (e,f) photospheric and chromospheric magnetic field strength, (g,h) magnetic field inclination in the background with an estimation of the azimuth (see the arrows). A fraction of the pixels have not been used in the inversion of He I 10830 Å triplet because the corresponding polarimetric signals are not above the prescribed threshold. (A color version of this figure is available in the online version.)

2006b,a; Centeno et al. 2009). The advantage of these spectral lines resides in the fact that they are almost absent in the quiet Sun and turn out to be relatively optically thin in the chromospheric and coronal structures where they originate.

Recently, Solanki et al. (2003) and Lagg et al. (2004) reconstructed loop-like structures that arrive to the corona by assuming that the He I 10830 Å triplet is formed within loops. Since the analysis carried out by these authors depend on a prior assumption,

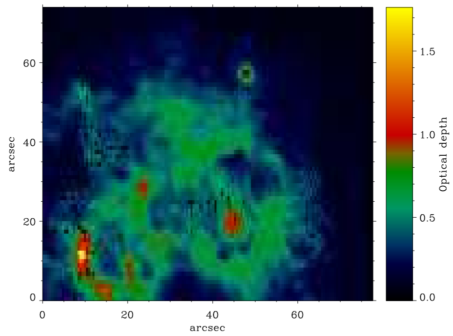

Fig. 2. Optical depth inferred at the center of the red component of the He I triplet. Note its similarity with the map of equivalent width shown in panel b of Fig. 1.

Judge (2009) has pointed out the possibility that the observations and the ensuing inferred magnetic field vector can be explained with simpler model assumptions: that the He I lines are formed in a corrugated surface at chromospheric heights in the active region atmosphere.

Observations of an emerging flux region carried out during September 27, 2007 with the TIP-II polarimeter mounted on the German VTT have been analyzed using the HAZEL[1] inversion code (Asensio Ramos et al. 2008) for the He I lines and the LILIA code (Socas-Navarro 2001) for the photospheric Si I line. The noise level is $\sim 6 \times 10^{-4}$ in units of the continuum intensity, which is only sufficient to detect the strongest Stokes Q and U signals in the red and blue components of the He I 10830 Å multiplet. Our chromospheric inversions are carried out using a one-component constant-properties slab illuminated from below by the photospheric radiation field, taking into account radiation transfer and magneto-optical effects and calculating the effect of the magnetic field on the energy levels under the incomplete Paschen-Back effect theory. The total computational time amounted to $\sim$ 72 hours in 4 processors, roughly 1–2 minutes per pixel.

[1] `http://www.iac.es/project/magnetism`

Figure 1 presents a comparison between the inferred photospheric and chromospheric physical parameters, together with the continuum image and the equivalent width (EW) map. The inversions show several interesting features. First, strong downflows are detected at positions compatible with the endpoints of the loop-like structures seen in the EW image, something already found by Solanki et al. (2003) and Lagg et al. (2004). Contrary to what they found, we do not clearly detect upflowing chromospheric material between the endpoints. Second, the inferred photospheric and chromospheric field strength maps are very similar in appearance, although in the chromospheric He I 10830 Å triplet we detect field strengths a factor 2 smaller on average than in the photospheric Si I line. Apart from this, the chromospheric field strength distribution appears to be smoother than the photospheric one, in accordance with the higher formation heights. Third, it is interesting to point out that the filamentary structures seen in the EW map do not present a significantly different magnetic field strength. However, according to the results presented in Fig. 2, there is a very good correlation between the optical depth inferred from the observations and the equivalent width. Consequently, the filamentary structure seen in the EW image must be produced by a density enhancement in a relatively uniform magnetic field. Fourth, the inclination of the field is such that there is a relatively rapid transition from one polarity to the other in the active region, both in the photosphere and in the chromosphere.

2. Some Bayesian considerations

The point raised by Judge (2009) about the interpretation of the results of Solanki et al. (2003) and Lagg et al. (2004) is important and should be analyzed more deeply. Using standard Bayesian ideas (see, e.g., Jaynes 2003), the problem is equivalent to that of comparing hypothesis H_0 (He I lines are formed in a loop) with hypothesis H_1 (He I lines are formed in a horizontal slab) for the explanation of a set of observations D. Model comparison should be carried out by calculating the ratio of posteriors for each hypothesis, which simplifies, thanks to the Bayes theorem, to the product of the ratio of evidences and the ratio of priors:

$$R = \frac{p(H_0|D)}{p(H_1|D)} = \frac{p(D|H_0)}{p(D|H_1)} \times \frac{p(H_1)}{p(H_0)}, \tag{1}$$

where

$$p(D|H) = \int p(D|\theta, H) p(\theta|M) \mathrm{d}\theta, \tag{2}$$

with θ the set of parameters defining model H. Whether or not hypothesis H_0 is to be preferred with respect to hypothesis H_1 can be established by the so-called "Jeffreys' scale" (see, e.g., Trotta 2008). We have weak evidence if $R \sim 3$, moderate evidence if $R \sim 12$ and strong evidence if $R \sim 150$, while it remains inconclusive if $R \lesssim 3$. Both hypotheses present the very same number of parameters and, in principle, both of them fit the data equally well, so that one could assume that both evidences are relatively similar. This demonstrates that, deciding whether He I lines are formed in a loop or in a horizontal slab is a matter of prior knowledge. It is justified to say that both models are equally probable because $R \sim 1$. Obviously, a way to overcome this situation is, as suggested by Judge (2009), to augment the problem with new data D, so that the ratio of evidences clearly favors one hypothesis. The reason is that, in such a case, one model would fit better the new observables (e.g., stereoscopic observations).

3. Additional complications and conclusions

As shown by Solanki et al. (2003), Lagg et al. (2004) and in the present work, the chromosphere of the observed region where weak He I absorption can be found is still magnetized. Consequently, even if loop-like structures reaching coronal heights exist, the interpretation of the polarimetric signals in terms of a slab of constant physical properties or in terms of a Milne-Eddington model is dubious and needs consideration. The reason is that, as shown in the upper panel of Fig. 3, we can encounter two situations: (a) one in which rays along the line-of-sight do not cross any loop and we see directly the chromosphere of the active region and (b) another one in which rays along the line-of-sight cross a loop before escaping.

We first focus on case (a) and analyze what happens as we move from one region with a given polarity to the other one with the opposite polarity. We assume that the chromosphere can be modeled as a constant properties slab whose magnetic field is either pointing upwards or downwards. The change in inclination is sharp at the central part of the slab and the field strength changes smoothly from 200 G at the center of each magnetic region to 50 G in the middle where the polarity reversal takes place. The input variation of the field strength and inclination with distance along the line joining the two polarities is shown in the lower panels of Fig. 3 (see the thin dashed lines). Using HAZEL, we synthesize the Stokes profiles emerging at each point assuming that the slab has an optical depth of $\Delta\tau = 0.3$ measured at the center of the red blended component of the He I 10830 Å multiplet. The field strength and inclination of the field are inferred using HAZEL keeping fixed the rest of parameters to the correct values. The blue solid curve in the lower left panel shows the inferred values in the case without noise, while the lower right panel presents the results when a noise level similar to our observations is added. We note that the inferred values are very close to the input ones, especially in the case without noise. In the noisy case, some fluctuations induce that the best fit in some points is achieved with a slightly larger field and a slightly more inclined field but the fundamental characteristics are recovered.

In case (b), the radiation escaping from the lower slab goes through a loop of optical depth $\Delta\tau = 0.6$. The magnetic field strength along the loop changes smoothly from 40 G close to the endpoints to 10 G in the central part. The inclination of the field is assumed to vary linearly, being horizontal at the top of the loop. The thin dot-dashed curves in the lower panels of Fig. 3 present such variations. Following the same strategy, we apply HAZEL to synthesize the emergent intensity and polarization

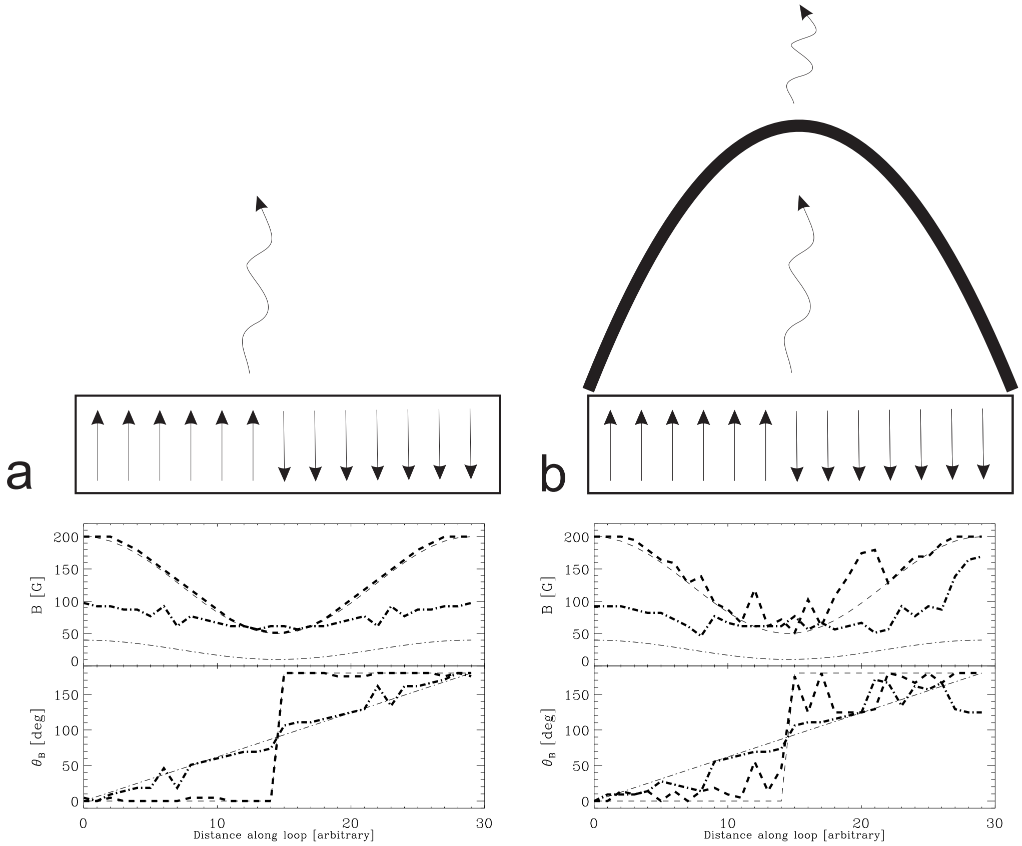

Fig. 3. Upper panels: sketch showing the two possible situations encountered when observing an emerging flux region with an active chromosphere and a loop, both producing He I absorption. Lower panels: input field strength and inclination, and the inferred ones using the inversion code HAZEL for the case without noise (lower left panel) and with a noise similar to our observations (lower right panel). The thin dashed lines show the input values for the chromospheric slab, while the thin dot-dashed present the input for the loop. The thick curves indicate what one infers from the observations in cases (a) and (b), respectively.

taking into account that the Stokes profiles entering the loop are those emerging from the lower slab. We apply HAZEL to infer the magnetic field vector from the synthetic observations and the results are shown in thick lines. For simplicity, we fix the total optical depth of the slab to $\Delta\tau = 0.9$. We have verified that this is the optical depth inferred from the synthetic observations if we leave this parameter free. Since we force HAZEL to interpret with only one field vector the combination of Stokes profiles produced by two completely different field distributions, the inferred magnetic field vector is somewhat between that in the lower slab and that in the loop, as indicated by the thick curves. Note that this happens even in the case without noise. As a consequence, if a loop producing absorption in He I is placed above an active region whose chromosphere also produces a significant absorption, one should be careful with the interpretation given to the inferred magnetic field vector.

Acknowledgements. Financial support by the Spanish Ministry of Science and Innovation through project AYA2007-63881 is gratefully acknowledged.

References

Asensio Ramos, A., Trujillo Bueno, J., & Landi Degl'Innocenti, E. 2008, ApJ, 683, 542
Bommier, V., Degl'Innocenti, E. L., Leroy, J.-L., & Sahal-Brechot, S. 1994, Sol. Phys., 154, 231
Casini, R. & Landi Degl'Innocenti, E. 2007, in Plasma Polarization Spectroscopy, ed. T. Fujimoto & A. B. S. Iwamae (Springer Verlag, Berlin-Heidelberg), 247
Casini, R., López Ariste, A., Tomczyk, S., & Lites, B. W. 2003, ApJ, 598, L67
Centeno, R., Collados, M., & Trujillo Bueno, J. 2006, ApJ, 640, 1153
Centeno, R., Trujillo Bueno, J., & Asensio Ramos, A. 2009, ApJ, in press
Harvey, J. & Hall, D. 1971, in Solar Magnetic Fields, ed. R. Howard (Reidel, Dordrecht), IAU Symp., 43, 279
Harvey, J. W. 2006, in Solar Polarization 4, ed. R. Casini & B. W. Lites, PASPC, 358, 419
Jaynes, E. T. 2003, in Probability Theory: The Logic of Science (Cambridge University Press, Cambridge)
Judge, P. G. 2009, A&A, 493, 1121
Lagg, A. 2007, Advances in Space Research, 39, 1734
Lagg, A., Woch, J., Krupp, N., & Solanki, S. K. 2004, A&A, 414, 1109
Landi Degl'Innocenti, E. 1982, Sol. Phys., 79, 291
Lin, H., Penn, M. J., & Kuhn, J. R. 1998, ApJ, 493, 978
López Ariste, A. & Casini, R. 2005, A&A, 436, 325
Merenda, L., Trujillo Bueno, J., Landi Degl'Innocenti, E., & Collados, M. 2006, ApJ, 642, 554
Querfeld, C. W., Smartt, R. N., Bommier, V., Landi Degl'Innocenti, E., & House, L. L. 1985, Sol. Phys., 96, 277
Ramelli, R., Bianda, M., Merenda, L., & Trujillo Bueno, T. 2006a, in Solar Polarization 4, PASPC, Vol. 358, ed. R. Casini & B. W. Lites, 448
Ramelli, R., Bianda, M., Trujillo Bueno, J., Merenda, L., & Stenflo, J. O. 2006b, in Solar Polarization 4, ed. R. Casini & B. W. Lites, PASPC, 358, 471
Rüedi, I., Keller, C. U., & Solanki, S. K. 1996, Sol. Phys., 164, 265
Socas-Navarro, H. 2001, in Advanced Solar Polarimetry: Theory, Observation and Instrumentation, ed. K. N. Nagendra & J. O. Stenflo, PASPC, 236, 487
Socas-Navarro, H. & Elmore, D. 2005, ApJ, 619, L195
Solanki, S. K., Lagg, A., Woch, J., Krupp, N., & Collados, M. 2003, Nature, 425, 692
Trotta, R. 2008, Contemporary Physics, 49, 71
Trujillo Bueno, J. 2009, in Magnetic Coupling between the Interior and the Atmosphere of the Sun, Astrophysics and Space Science Proceedings, ed. S. S. Hasan & R. J. Rutten (Springer Verlag, Heidelberg)
Trujillo Bueno, J., Landi Degl'Innocenti, E., Collados, M., Merenda, L., & Manso Sainz, R. 2002, Nature, 415, 403
Trujillo Bueno, J., Merenda, L., Centeno, R., Collados, M., & Landi Degl'Innocenti, E. 2005, ApJ, 619, L191